Monthly Notices of the ROYAL ASTRONOMICAL SOCIETY

MNRAS **501,** 4110–4122 (2021) doi:10.1093/mnras/staa3937
Advance Access publication 2020 December 24

Intra-night optical variability of γ-ray detected narrow-line Seyfert1 galaxies

Vineet Ojha [1]★ Hum Chand [1,2]★ and Gopal-Krishna [1,3]

[1] *Aryabhatta Research Institute of Observational Sciences (ARIES), Manora Peak, Nainital 263002, India*
[2] *Department of Physics and Astronomical Sciences, Central University of Himachal Pradesh (CUHP), Dharamshala 176215, India*
[3] *UM-DAE Centre for Excellence in Basic Sciences, Vidyanagari, Mumbai 400098, India*

Accepted 2020 December 17. Received 2020 December 15; in original form 2020 May 29

ABSTRACT

We report the first attempt to systematically characterize intra-night optical variability (INOV) of the rare and enigmatic subset of narrow-line Seyfert1 galaxies (NLSy1s), which is marked by detection in the γ-ray band and is therefore endowed with Doppler-boosted relativistic jets, like blazars. However, the central engines in these two types of AGN are thought to operate in different regimes of accretion rate. Our INOV search in a fairly large and unbiased sample of 15 γ-ray NLSy1s was conducted in 36 monitoring sessions, each lasting $\geq$3 h. In our analysis, special care has been taken to address the possible effect on the differential light curves, of any variation in the seeing disc during the session, since that might lead to spurious claims of INOV from such AGN due to the possibility of a significant contribution from the host galaxy to the total optical emission. From our observations, a duty cycle (DC) of INOV detection in the γ-ray NLSy1s is estimated to be around 25–30 per cent, which is comparable to that known for blazars. This estimate of DC will probably need an upward revision, once it becomes possible to correct for the dilution of the AGN's non-thermal optical emission by the (much steadier) optical emission contributed not only by the host galaxy but also the nuclear accretion disc in these high Eddington rate accretors. Finally, we also draw attention to the possibility that sharp optical flux changes on sub-hour time-scale are less rare for γ-ray NLSy1s, in comparison to blazars.

Key words: surveys – galaxies: active – galaxies: jets – galaxies: Seyfert – gamma-rays: galaxies.

1 INTRODUCTION

The diversity of intensity variations across the electromagnetic spectrum is a prominent characteristic of active galactic nuclei (AGNs) and it has been extensively leveraged to probe their emission mechanisms occurring on physical scales that are currently inaccessible to direct imaging by any available technique (e.g. Urry & Padovani 1995; Wagner & Witzel 1995; Ulrich, Maraschi & Urry 1997; Zensus 1997). AGN variability on minutes to hour-like time-scales in the optical waveband is termed as intra-night optical variability (INOV; Gopal-Krishna, Wiita & Altieri 1993). Such variations have proved particularly useful for probing and characterizing the jet activity in blazars and radio-loud narrow-line Seyfert 1 (NLSy1) galaxies, as well as for identifying any blazar-like signatures in radio-quiet AGNs (e.g. Miller, Carini & Goodrich 1989; Gopal-Krishna et al. 1993; Gopal-Krishna, Sagar & Wiita 1995; Jang & Miller 1995; Heidt & Wagner 1996; Bai et al. 1999; Romero, Cellone & Combi 1999; Fan, Qian & Tao 2001; Stalin et al. 2004; Gupta & Joshi 2005; Carini et al. 2007; Ramírez et al. 2009; Goyal et al. 2012, 2013; Kumar et al. 2017; Ojha, Gopal-Krishna & Chand 2019; Paliya 2019). In the case of blazars, INOV is generally associated with disturbances within their relativistic jets, e.g. the well-known 'shock-in-jet' model (e.g. see Marscher & Gear 1985; Hughes, Aller & Aller 1991; Qian et al. 1991; Wagner & Witzel 1995; Marscher 1996). However, helicity, precession, or other geometrical effects associated with the jets (e.g. see Camenzind & Krockenberger 1992; Gopal-Krishna & Wiita 1992), perhaps linked to short-term instabilities on the surface of the accretion disc but propagated into the relativistic effects jets, have also been considered as possible mechanisms for INOV in blazars (e.g. see Chakrabarti & Wiita 1993; Mangalam & Wiita 1993; also Czerny et al. 2008).

As recently summarized in Gopal-Krishna & Wiita (2018), prominent among the radio-quiet AGNs covered extensively in INOV studies are radio-quiet Seyfert galaxies (Carini, Noble & Miller 2003), radio-quiet quasars (Gopal-Krishna et al. 2003), and weak emission-line quasars (Gopal-Krishna, Joshi & Chand 2013; Chand, Kumar & Gopal-Krishna 2014; Kumar, Gopal-Krishna & Chand 2015; Kumar, Chand & Gopal-Krishna 2016; Kumar et al. 2017). A possible cause for the low-level INOV detections in some such cases is the transient formation of micro-arcsec scale, probably in poorly aligned optical synchrotron jets (see Gopal-Krishna et al. 2003; Stalin et al. 2004). The possibility that misaligned relativistic jets could be hidden among radio-quiet AGNs has also been noted in the context of NLSy1 galaxies (e.g. Foschini 2011; Berton et al. 2018). None the less, INOV studies of these (low-luminosity) AGNs continue to be sparse and have been limited to a small data set (Miller et al. 2000; Ferrara et al. 2001; Klimek, Gaskell & Hedrick 2004; Liu et al. 2010; Paliya et al. 2013a; Kshama, Paliya & Stalin 2017; Ojha, Chand & Gopal-Krishna 2018; Paliya 2019; Ojha et al. 2020b), even though they were discovered over three decades ago (Osterbrock & Pogge 1985) and basically defined by

★ E-mail: vineetojhabhu@gmail.com (VO); humchand@gmail.com (HC)

the rather small width of the optical Balmer emission lines, with full width at half-maximum (FWHM) being < 2000 km s^{-1} for Hβ (Osterbrock & Pogge 1985; Goodrich et al. 1989), stronger permitted Fe II, and weak [O III] emission lines such that the flux ratio of [O III] λ5007/Hβ is < 3 (Shuder & Osterbrock 1981). With some possible exceptions, they also show strong [Fe VII] and [Fe X] emission lines (see, however, Pogge 2011; Cracco et al. 2016). In addition to a soft X-ray spectrum (Boller, Brandt & Fink 1996; Wang, Brinkmann & Bergeron 1996; Grupe et al. 1998), they are also known to display rapid X-ray (and sometimes even optical) flux variability (e.g. Leighly 1999; Komossa & Meerschweinchen 2000; Miller et al. 2000; Klimek et al. 2004; Liu et al. 2010; Paliya et al. 2013a; Kshama et al. 2017; Ojha et al. 2019). Observational evidence, as reviewed recently in Paliya (2019), suggests that this class of AGN harbour relatively less massive black holes (10^6–10^8 M$_\odot$; Grupe & Mathur 2004; Deo, Crenshaw & Kraemer 2006; Peterson 2011), which are accreting at a high fraction of the Eddington rate, in contrast to quasars (e.g. Peterson et al. 2000). Interestingly, NLSy1 galaxies (NLSy1s) exhibit the radio-loud/radio-quiet bimodality, displayed by QSOs, and thus are radio-quiet in most cases (Kellermann et al. 2016, and references). Only about ~ 7 per cent of NLSy1s are radio-loud with the radio-loudness parameter[1] $R_{5\,\mathrm{GHz}} > 10$ (Komossa et al. 2006; Zhou et al. 2006; Rakshit et al. 2017; Singh & Chand 2018). For $R_{5\,\mathrm{GHz}} > 100$, the fraction drops further to just 2–3 per cent (see also Komossa et al. 2006, Zhou & Wang 2002; Yuan et al. 2008).

It may be noted that the inference about NLSy1s having relatively less massive black holes (BHs), although not uncontested (e.g. Decarli et al. 2008; Marconi et al. 2008; Calderone et al. 2013; Viswanath et al. 2019), appears none the less to be favoured by the weight of evidence, as summarized in Paliya (2019). A crucial implication then would be that the jet activity in NLSy1s is powered by central engines that operate significantly differently from those in quasars and their blazar subset. It is therefore remarkable that the jetted NLSy1s (see below) and blazars engender very similar manifestations of their relativistic jets, such as superluminal motion (see, e.g. Lister 2018), a double-humped spectral energy distribution (e.g. Abdo et al. 2009c; Paliya et al. 2013b; Paliya 2019), and violent optical and infrared flux variability (Liu et al. 2010; Itoh et al. 2013; Maune, Miller & Eggen 2013; Paliya et al. 2013a). This makes it especially desirable to search for any contrasting observational properties between blazars and the jetted NLSy1s. In this study, we pursue this objective from the standpoint of rapid optical flux variability, i.e. INOV, which is now believed to be a key attribute associated with blazar-type AGN (see, e.g. Goyal et al. 2013; Gopal-Krishna & Wiita 2018; Gopal-Krishna, Britzen & Wiita 2019).

It is noteworthy that in the case of NLSy1 galaxies, radio emission from star formation process alone could sometimes lead to a radio-loud classification, even if a relativistic jet is not present (Ganci et al. 2019). Therefore, a conclusive evidence that NLSy1s are capable of ejecting relativistic jets emerged only from the rather unexpected discovery of γ-ray emission from a handful of NLSy1s, using the *Fermi*-Large Area Telescope (*Fermi*-LAT)[2] (Abdo et al. 2009a,b,c; Foschini et al. 2010; Foschini 2011; D'Ammando et al. 2012, 2015; Yao et al. 2015; Paliya et al. 2018; Yang et al. 2018; Yao et al. 2019). Since then, the number of such NLSy1s has slowly increased to just about 20 (Paliya 2019), confirming their rarity. Hereinafter, we shall refer to such AGN as γ-ray NLSy1.

In fact, almost a decade prior to their detection of NLSy1s in γ-rays, INOV had already been detected from a few NLSy1s (Miller et al. 2000; Ferrara et al. 2001; Klimek et al. 2004). The first INOV detection in a *Fermi*/LAT-detected NLSy1 galaxy was for J094857.30+002224.0, for which Liu et al. (2010) observed a huge INOV amplitude of ~ 0.5 mag. This source is known to exhibit strong optical variability on longer time-scales as well (Maune et al. 2013). None the less, as an AGN class, γ-ray NLSy1s are marked by rather poorly known INOV characteristics, primarily because INOV observations have so far been reported for just 6[3] of them (Liu et al. 2010; Paliya et al. 2013a, 2016; Kshama et al. 2017; Ojha et al. 2019, 2020b). Therefore, the primary aim of this study is to bridge this knowledge gap, by determining the INOV characteristics of this rare and enigmatic class of AGN. For this, we use a much larger sample, now possible to assemble, and employ a single telescope, as well as a uniform analysis procedure for the entire sample.

This paper is structured as follows. In Section 2, we outline the sample selection procedure. Section 3 provides details of our intra-night optical monitoring and the data reduction procedure. The statistical analysis is presented in Section 4 and our main results followed by a brief discussion are given in Section 5. In Section 6, we summarize our main conclusions.

2 THE SAMPLE

The present sample is a well-defined, large subset of the compilation of all 22 NLSy1s reported to have a γ-ray detection (Paliya 2019). Our first filter, namely a γ-ray detection threshold of $>3\sigma$, led to the rejection of the sources J124634.65+023809.1 and J142106.00+385522.5 (see Foschini 2011; Paliya et al. 2018). A third source, J200755.18–443444.3, got excluded because its low declination precludes monitoring from our observatory. Out of the remaining 19 sources, another two, namely J110223.37+223920.5 and J164100.1+345453.0, were rejected since their reported γ-ray detections have not been confirmed by Foschini et al. (2015) and Ciprini & Fermi-LAT Collaboration (2018). Note that these two sources are also not contained in the *Fermi* Large Area Telescope Fourth Source Catalog (Abdollahi et al. 2020). The sixth source to be excluded is J003159.9+093618.0, since Paliya (2019) suggests it to be a probable counterpart of the unidentified γ-ray source 3FGL J003159+093615. The last source to be excluded is 3C 286 (J133108.3+303032.0); unlike all other γ-ray detected NLSy1s, its radio spectrum is steep and it has been argued that its γ-ray emission may substantially originate outside the jet (Berton et al. 2018). The final sample of 15 γ-ray NLSy1s is listed in Table 1.

3 OBSERVATIONS AND DATA REDUCTION

3.1 Photometric monitoring observations

All 15 γ-ray NLSy1s in our sample were monitored in the broad-band filter *R*, with the 1.3-metre (m) Devasthal Fast Optical Telescope (DFOT) located at Devasthal near Nainital (Sagar et al. 2010) and operated by the Aryabhatta Research Institute of Observational

[1]Radio loudness is usually parametrized by the ratio (R) of the rest-frame flux densities at 5 GHz and 4400 Å, being $R \leq 10$ and > 10 for radio-quiet and radio-loud quasars, respectively (e.g. see Stocke et al. 1992; Visnovsky et al. 1992; Kellermann et al. 1994, 1989).

[2]https://heasarc.gsfc.nasa.gov/docs/heasarc/missions/fermi.html.

[3]We exclude the NLSy1 galaxy J110223.37+223920.5, with $< 3\sigma$ detection in γ-rays (Foschini et al. 2015), whose INOV observations are reported by Ojha et al. (2020b).

Table 1. The present sample of 15 γ-ray detected NLSy1 galaxies.

SDSS name (1)	R mag (2)	z (3)	$R_{1.4\,\mathrm{GHz}}$ (4)
J032441.20+341045.0	13.10	0.06	318[a]
J084957.98+510829.0	17.79	0.58	4496[a]
J093241.15+530633.8	18.82	0.60	19 188
J093712.33+500852.1	18.88	0.28	2007
J094635.07+101706.1	18.90	1.00	11 731
J094857.32+002225.6	18.17	0.58	846[a]
J095820.90+322401.6	15.51	0.53	1786
J122222.99+041315.9	17.06	0.97	1534[a]
J130522.75+511640.2	15.80	0.79	509
J144318.56+472556.7	17.70	0.70	1921
J150506.48+032630.8	17.72	0.41	3364[a]
J152039.70+421111.0	18.09	0.48	42 908
J164442.53+261913.3	16.60	0.14	447[a]
J211817.40+001316.8	18.60	0.46	12 410
J211852.90–073229.3	19.48	0.26	4664

Columns are as follows: (1) SDSS name of the sources; (2) R-band magnitude, taken from Monet (1998); (3) emission-line redshift, taken from Paliya et al. (2019); and (4) $R_{1.4\,\mathrm{GHz}} \equiv f_{1.4\,\mathrm{GHz}}/f_{4400\,\text{Å}}$, estimated by taking the rest-frame 1.4-GHz flux density from Paliya (2019) and the optical flux density at rest-frame 4400 Å, estimated by fitting the SDSS spectrum, following the procedure described in Rakshit et al. (2017). [a]Values of $R_{1.4\,\mathrm{GHz}}$ taken from Foschini (2011), except for J164442.53+261913.3 for which the value is taken from Yuan et al. (2008) and J122222.99+041315.9 for which $R_{1.4\,\mathrm{GHz}}$ has been estimated using its core flux density of 0.6 Jy at 1.4 GHz from Yuan et al. (2008).

Sciences (ARIES), India. The DFOT is a Ritchey–Chretien (RC) telescope with a fast beam (f/4) and has a pointing accuracy better than 10 arcsec rms. It is equipped with a 2k×2k deep thermoelectrically cooled (to about −85°C) Andor CCD camera, has a pixel size of 13.5 microns, a plate scale of 0.53 arcsec per pixel, giving a field of view (FOV) of ∼18 × 18 arcmin^2 on the sky. The detector chip, having a system rms noise and gain of 7.5 e^- and 2.0 e^- ADU^{-1}, respectively, was read out at the speed of 1 MHz. Each target AGN was monitored for a duration between 3.0 to 5.5 h, as is usual for our INOV campaigns, with the aim to enhance the probability of INOV detection (see Carini 1990). Also, in order to strengthen the INOV statistics, each of our 15 γ-ray NLSy1s was monitored at least in two intra-night sessions, the solitary exception being the source J093712.33+500852.1 for which bad weather restricted the monitoring to a single successful session. The exposure time for each science frame was set between 4 and 20 min, depending on the brightness of the AGN, the sky transparency, and the lunar phase. The typical median seeing (FWHM of the point spread function (PSF)) during our monitoring sessions ranged between ∼ 2 and 3 arcsec.

3.2 Data reduction

Pre-processing of the raw frames was done by performing the bias subtraction, flat-fielding, and cosmic ray removal using the standard tasks within the IRAF[4] software package. Instrumental magnitudes of the target NLSy1 and the two chosen comparison stars registered in the CCD frames were measured by aperture photometry (Stetson 1987, 1992), using the DAOPHOT II algorithm.[5] A key parameter for photometry is the aperture size, used for measuring the instrumental magnitude and the corresponding signal-to-noise ratio (S/N) of the individual photometric data points. As reported in Howell (1989), S/N is maximized when the photometric aperture radius is approximately equal to the FWHM of the seeing disc, i.e. point spread function (PSF). However, we note that the situation can be more complex while dealing with some relatively nearby AGNs (e.g. two sources in our sample, viz., J032441.20+341045.0 at z = 0.06; J164442.53+261913.3 at z = 0.14) because a significant contribution to the total flux can come from the underlying host galaxy and hence the relative contributions of the (point-like) AGN and the host galaxy to the aperture photometry can vary significantly as the PSF changes during the session. As emphasized by Cellone, Romero & Combi (2000), the standard analysis of the differential light curves (DLCs) could then lead to statistically significant, yet spurious claims of INOV for small apertures comparable to the PSF. Keeping this caution in mind, we have first estimated the PSF (FWHM) for each CCD frame (by averaging the profiles of five bright although clearly unsaturated stars in that frame) and treating the median of those values as the PSF (i.e. FWHM) for that session. The photometry was then performed taking four values of aperture radius, viz., 1×FWHM, 2×FWHM, 3×FWHM, and 4×FWHM. The resulting DLCs of the target AGN were compared with the observed trend of variation of the seeing disc (FWHM) during the session, before proceeding with a quantitative analysis. In practice, this turned out to be an extra cautious approach since, except for three sessions (dated: 2019 April 25, 2019 May 4, and 2020 March 22; see Figs 3 and 4), FWHM remained quite steady, (variations mostly within an arcsec), without showing any systematic trend during the session. Under this circumstance, an aperture radius of 2×FWHM is expected to yield fairly reliable DLCs for the target AGN, even if its host galaxy is up to 2 mag brighter than the AGN (see table 2 of Cellone et al. 2000).

As an additional check for a significant host-galaxy contribution to our aperture photometry, we have fitted the brightness profile of a bright (unsaturated) star, placed at the position of our target AGN. The brightness of the star was varied while keeping the FWHM unchanged. The latter was determined by taking the median of the values measured for nearby 10 bright (unsaturated) stars within the same CCD frame. The best-fitting profile obtained was then subtracted out from the target image, to get the residual image. The counts in the residual image were found to be comparable to the sky background counts for all our sources, except for J032441.20+341045.0 with the highest significance reaching 2.13σ for the monitoring session dated 2016 November 23. Note that this AGN is a low-redshift NLSy1 galaxy (z = 0.06), and is already known to have a clearly visible host galaxy, as discussed in details by Ojha et al. (2019). This basic trend emerging from the model-fitting is in accord with the findings of the recent search for host galaxy emission for NLSy1 galaxies (Olguín-Iglesias, Kotilainen & Chavushyan 2020). We note that nine of our NLSy1s are in fact common to their sample and they could detect host galaxies of just 4 of them, which are also the nearest ($z \lesssim 0.6$) ones in their sample. And this is in spite of their using a far more sensitive telescope (the 8.6-m ESO Very Large Telescope (VLT)) than ours and taking much longer exposures (median 1800 s) than we took (median 540 s) in our observations for our current sample with the 1.3-m DFOT.

[4]Image Reduction and Analysis Facility (http://iraf.noao.edu/).

[5]Dominion Astrophysical Observatory Photometry (http://www.astro.wisc.edu/sirtf/daophot2.pdf).

Additional comments on some individual cases including this low-redshift source are provided in Section 5.

For each session, DLCs of the target NLSy1 were derived relative to two (steady) comparison stars which were chosen on the basis of their proximity to the target AGN in brightness, the importance of which for a reliable INOV detection has been highlighted by Howell, Warnock & Mitchell (1988) and further emphasized in Cellone, Romero & Araudo (2007). For eight sources of our sample, we were able to find at least one comparison star which falls within ∼1 mag of the target AGN. The magnitude offsets (Δm_R) for the remaining sources are also not large, namely 2.0 (J093241.15+530633.8), 1.57 (J094635.07+101706.1), 1.26 (J130522.75+511640.2), 1.29 (J144318.60+472557.0), 1.53 (J152039.70+421111.00), 1.54 (J164442.53+261913.3), and 1.40 mag (J211817.40+001316.8). The coordinates and other parameters of the comparison stars used for the different sessions are given in Table 2 for our entire set of 15 γ-ray NLSy1s. The SDSS $g-r$ colours for the target NLSy1 and their chosen comparison stars are: <0.82 and <1.80 in all cases, with the median values being 0.30 and 0.70, respectively (column 7 in Table 2). It has been demonstrated by Carini et al. (1992) and Stalin et al. (2004) that colour differences of this order should produce a negligible effect on the DLCs as the atmospheric attenuation varies during a session.

4 STATISTICAL ANALYSIS

To search for the presence/absence of INOV in a DLC, we have employed two different forms of the *F-test* proposed by de Diego (2010). These are (i) the standard F-test (hereafter F^{η}-test; e.g. see Goyal et al. 2012) and (ii) the power-enhanced *F-test* (hereafter $F_{\rm enh}$-test; e.g. see de Diego 2014). Detailed description of these two tests is given in our previous papers (Ojha et al. 2019, 2020b, and references therein).

In brief, following Goyal et al. (2012), F^{η}-test can be written as

$$F_1^{\eta} = \frac{\sigma^2_{(q-s1)}}{\eta^2\left\langle\sigma^2_{q-s1}\right\rangle}, \qquad F_2^{\eta} = \frac{\sigma^2_{(q-s2)}}{\eta^2\left\langle\sigma^2_{q-s2}\right\rangle}, \tag{1}$$

where $\sigma^2_{(q-s1)}$ and $\sigma^2_{(q-s2)}$ are the variances with $\langle\sigma^2_{q-s1}\rangle = \sum_{i=1}^{N}\sigma^2_{i,\,err}(q-s1)/N$ and $\langle\sigma^2_{q-s2}\rangle$ being the mean square (formal) rms errors of the individual data points in the 'target AGN − comparison star1' and 'target AGN − comparison star2' DLCs, respectively. The parameter η is the error scaling factor and is taken to be 1.5 from Goyal et al. (2012) (see Ojha et al. 2020b). The DLCs of the target AGN relative to the two comparison stars and the 'star-star' DLCs are displayed in the second, third, and fourth panels from the bottom in Figs 1–4, respectively.

For this study, we have set two critical significance levels, $\alpha = 0.01$ and 0.05, which correspond to the confidence levels of 99 and 95 per cent, respectively. The F-values, obtained for individual DLCs using equation (1), were compared with the adopted critical F-value (F_c), and an NLSy1 is deemed to be variable only if the F-values computed for both its DLCs are above the critical F value at 99 per cent confidence level (hereafter $F_c(0.99)$). The computed F^{η}-values and the correspondingly inferred variability status for the 36 sessions devoted to the 15 γ-ray NLSy1s are given in columns 6 and 7 of Table 3.

The $F_{\rm enh}$-test, as described in Ojha et al. (2020b) can be written as

$$F_{\rm enh} = \frac{s^2_{\rm qso}}{s^2_{\rm stc}}, \qquad s^2_{\rm stc} = \frac{1}{\left(\sum_{j=1}^{k}N_j\right)-k}\sum_{j=1}^{k}\sum_{i=1}^{N_j}s^2_{j,i}, \tag{2}$$

where $s^2_{\rm qso}$ is the variance of the DLC of the target AGN and the reference star (the one matching better in magnitude to the target AGN out of the two chosen comparison stars), while $s^2_{\rm stc}$ is the stacked variance of the DLCs of the comparison stars and the reference star (de Diego 2014). N_j is the number of observations of the jth star and k is the total number of comparison stars.

The $s^2_{j,i}$ is the scaled square deviation defined as

$$s^2_{j,i} = \omega_j(m_{j,i} - \bar{m}_j)^2, \tag{3}$$

where $m_{j,i}$'s are the differential instrumental magnitudes, and $\bar{m}_j$ is the mean differential magnitude of the reference star and the jth comparison star. The scaling factor ω_j (see also Joshi et al. 2011) is taken as

$$\omega_j = \frac{\left\langle\sigma^2_{i,\rm err}(q-ref)\right\rangle}{\left\langle\sigma^2_{i,\rm err}(s_j-ref)\right\rangle}. \tag{4}$$

The $F_{\rm enh}$ value is estimated using equation (2) and compared with its $F_c(0.99)$ and $F_c(0.95)$. An NLSy1 is considered variable (V) and probable variable (PV) if the computed values of 'NLSy1-reference star' DLC are found to be as $F_{\rm enh} > F_c(0.99)$ and $F_c(0.95) < F_{\rm enh} \leq F_c(0.99)$, respectively. The estimated $F_{\rm enh}$-values and the corresponding variability status for the 15 γ-ray NLSy1s are given in columns 8 and 9 of Table 3.

4.1 Estimation of the INOV DC and amplitude

For computing the DC of INOV in our sample of 15 γ-ray NLSy1s, we have followed the definition given by Romero et al. (1999):

$$DC = 100\frac{\sum_{j=1}^{n}F_j(1/\Delta t_j)}{\sum_{j=1}^{n}(1/\Delta t_j)}\ \text{per cent}, \tag{5}$$

where $\Delta t_j = \Delta t_{j,\,\rm obs}(1+z)^{-1}$ is the actual duration of the jth monitoring session, corrected for the target AGN's redshift, z (see details in Ojha et al. 2019, 2020b). F_j is set equal to 1 if INOV is detected, otherwise F_j is taken to be zero. Secondly, in order to prevent the DC estimate from getting biased towards more frequently monitored sources in the sample, we have chosen to select just two sessions per source for calculating DC, even though data are available for more sessions (Table 3). The selection of the two sessions was kept unbiased, by basing it on the monitoring duration (T) and thus the longest two sessions were selected, as shown by placing the session dates within parentheses on the panels in Figs 1–4 and also in Table 3. The computed values for the sample of 15 γ-ray NLSy1, using the two different statistical tests are tabulated in Table 4.

For estimating the amplitude of INOV (ψ) of the monitored AGN, which quantifies its variation in a given session, we followed the definition given by Heidt & Wagner (1996):

$$\psi = \sqrt{(A_{\rm max} - A_{\rm min})^2 - 2\sigma^2}, \tag{6}$$

with $A_{\rm min,\,max}$ = minimum (maximum) values in the 'target AGN − star' DLC and $\sigma^2 = \eta^2\langle\sigma^2_{q-s}\rangle$, where, $\langle\sigma^2_{q-s}\rangle$ is the mean square (formal) rms errors of individual data points and $\eta = 1.5$ (Goyal et al. 2012).

5 RESULTS AND DISCUSSION

As mentioned in Section 1, the present INOV study based on a sample of 15 γ-ray NLSy1 galaxies represents a substantial advance over the previous reports of INOV properties of this rather poorly understood class of AGN. Those earlier investigations were based on just a handful (six) of AGNs in this class. Recall that just two

Table 2. The observational log and basic parameters of the comparison stars used for the sample of 15 γ-ray NLSy1 galaxies.

Target AGN and the comparison stars (1)	Date(s) of monitoring (2)	RA (J2000) ($^{h\,m\,s}$) (3)	Dec. (J2000) ($^{\circ}\,'\,''$) (4)	g (mag) (5)	r (mag) (6)	$g-r$ (mag) (7)
J032441.20+341045.0	2016 Nov 22, 23; Dec 2; 2017 Jan 3, 4	03 24 41.20	+34 10 45.00	[a]	[a]	[a]
S1		03 24 53.68	+34 12 45.62	[a]	[a]	[a]
S2		03 24 53.55	+34 11 16.58	[a]	[a]	[a]
J084957.98+510829.0	2017 Dec 13, 2019 Apr 8	08 49 57.98	+51 08 29.04	18.92	18.28	0.64
S1		08 50 12.62	+51 08 08.03	19.45	18.06	1.39
S2		08 50 03.07	+51 09 12.23	17.82	17.09	0.73
J093241.15+530633.8	2019 Jan 13, 2020 Apr 11	09 32 41.15	+53 06 33.79	18.90	18.84	0.06
S1	2019 Jan 13	09 32 17.61	+53 01 48.66	19.73	18.21	1.52
S2	2019 Jan 13	09 32 41.51	+53 06 14.10	18.72	17.50	1.22
S3	2020 Apr 11	09 32 12.62	+53 09 09.46	17.86	16.82	1.04
S4	2020 Apr 11	09 31 53.14	+53 01 30.54	16.88	16.21	0.67
J093712.33+500852.1	2019 Mar 23	09 37 12.33	+50 08 52.14	19.53	18.79	0.74
S1		09 38 01.04	+50 08 49.80	18.36	17.84	0.52
S2		09 36 34.62	+50 09 56.10	18.45	17.07	1.38
J094635.07+101706.1	2019 Dec 26, 29	09 46 35.07	+10 17 06.13	19.51	19.21	0.30
S1	2019 Dec 26, 29	09 46 50.04	+10 10 13.97	18.25	17.71	0.54
S2	2019 Dec 26	09 46 35.29	+10 11 40.29	18.02	17.64	0.38
S3	2019 Dec 29	09 47 04.35	+10 15 52.01	18.72	18.03	0.69
J094857.32+002225.6	2016 Dec 2; 2017 Dec 21	09 48 57.32	+00 22 25.56	18.59	18.43	0.16
S1		09 48 36.95	+00 24 22.55	17.69	17.28	0.41
S2		09 48 37.47	+00 20 37.02	17.79	16.70	1.09
J095820.90+322401.6	2019 Jan 8; Feb 16	09 58 20.90	+32 24 01.60	16.01	16.00	0.01
S1		09 58 18.30	+32 28 34.43	15.80	15.31	0.49
S2		09 58 35.20	+32 28 19.27	15.50	15.07	0.43
J122222.99+041315.9	2017 Jan 3, 4; Feb 21, 22; Mar 4, 24	12 22 22.99	+04 13 15.95	17.02	16.80	0.22
S1		12 22 34.02	+04 13 21.57	18.63	17.19	1.44
S2		12 21 56.12	+04 15 15.19	17.22	16.78	0.44
J130522.75+511640.2	2017 Apr 4; 2019 Apr 25	13 05 22.74	+51 16 40.26	17.29	17.10	0.19
S1	2017 Apr 04	13 06 16.16	+51 19 03.67	16.96	15.92	1.04
S2	2017 Apr 4; 2019 Apr 25	13 05 57.57	+51 11 00.97	16.35	15.26	1.09
S3	2019 Apr 25	13 05 44.25	+51 07 35.85	17.88	16.42	1.46
J144318.56+472556.7	2018 Mar 11, 23	14 43 18.56	+47 25 56.74	18.14	18.17	−0.03
S1		14 43 37.14	+47 23 03.03	17.51	16.82	0.69
S2		14 43 19.05	+47 19 00.98	18.03	16.75	1.28
J150506.48+032630.8	2017 Mar 25; 2018 Apr 12	15 05 06.48	+03 26 30.84	18.64	18.22	0.42
S1		15 05 32.05	+03 28 36.13	18.13	17.64	0.49
S2		15 05 14.52	+03 24 56.17	17.51	17.14	0.37
J152039.70+421111.0	2019 May 5, 2020 Mar 22	15 20 39.70	+42 11 11.19	19.31	18.94	0.37
S1	2019 May 05	15 20 42.81	+42 07 28.32	19.43	18.03	1.40
S2	2019 May 05	15 21 20.78	+42 03 20.45	17.51	17.09	0.42
S3	2020 Mar 22	15 21 11.63	+42 11 45.71	17.89	17.08	0.81
S4	2020 Mar 22	15 20 57.17	+42 10 04.87	18.13	16.68	1.45
J164442.53+261913.3	2017 Apr 3; 2019 Apr 26	16 44 42.53	+26 19 13.3	18.03	17.61	0.42
S1		16 45 20.03	+26 20 54.55	16.56	15.89	0.67
S2		16 44 34.40	+26 15 30.27	16.28	15.80	0.48
J211817.40+001316.8	2019 Jun 7, 10	21 18 17.40	+00 13 16.76	18.71	18.45	0.26
S1	2019 Jun 7, 10	21 18 36.48	+00 08 35.40	18.48	17.78	0.70
S2	2019 Jun 07	21 18 03.72	+00 06 45.79	17.99	17.41	0.58
S3	2019 Jun 10	21 18 10.06	+00 15 30.61	17.99	17.63	0.36
J211852.90–073229.3	2018 Oct 4; 2019 Jun 9	21 18 52.90	−07 32 29.34	18.78	17.96	0.82
S1		21 18 25.68	−07 31 20.72	17.83	17.28	0.55
S2		21 18 52.33	−07 31 37.64	17.78	16.88	0.90

Columns are listed as follows: (1) Target AGN and the comparison stars; (2) date(s) of monitoring; (3) Right Ascension; (4) Declination; (5) SDSS g-band magnitude; (6) SDSS r-band magnitude; (7) SDSS '$g-r$' colours. The positions and apparent magnitudes of the sources and their comparison stars were taken from the SDSS DR14 (Abolfathi et al. 2018). Due to the non-availability of the SDSS '$g-r$' colours for the source, J032441.20+341045.0, and its comparison stars (marked by '[a]' in columns 5–7), '$B-R$' colours have been used from USNO-A2.0 catalogue (Monet 1998) with B magnitude as 14.50 (target AGN), 15.60 (S1), 16.20 (S2) and R magnitude as 13.70 (target AGN), 14.40 (S1), 14.40 (S2).

out of all the NLSy1s currently known to have a confirmed ($>3\sigma$) detection in γ-rays have been left out of the present sample, on grounds well justified in Section 2. Thus, we believe that the INOV characterization presented here should be fairly representative of this intriguing class of jetted AGN. This characterization would also enable their systematic comparison with the already well established INOV properties of the blazar type AGN whose relativistic jets are not only more powerful, on the whole, but also thought to form under

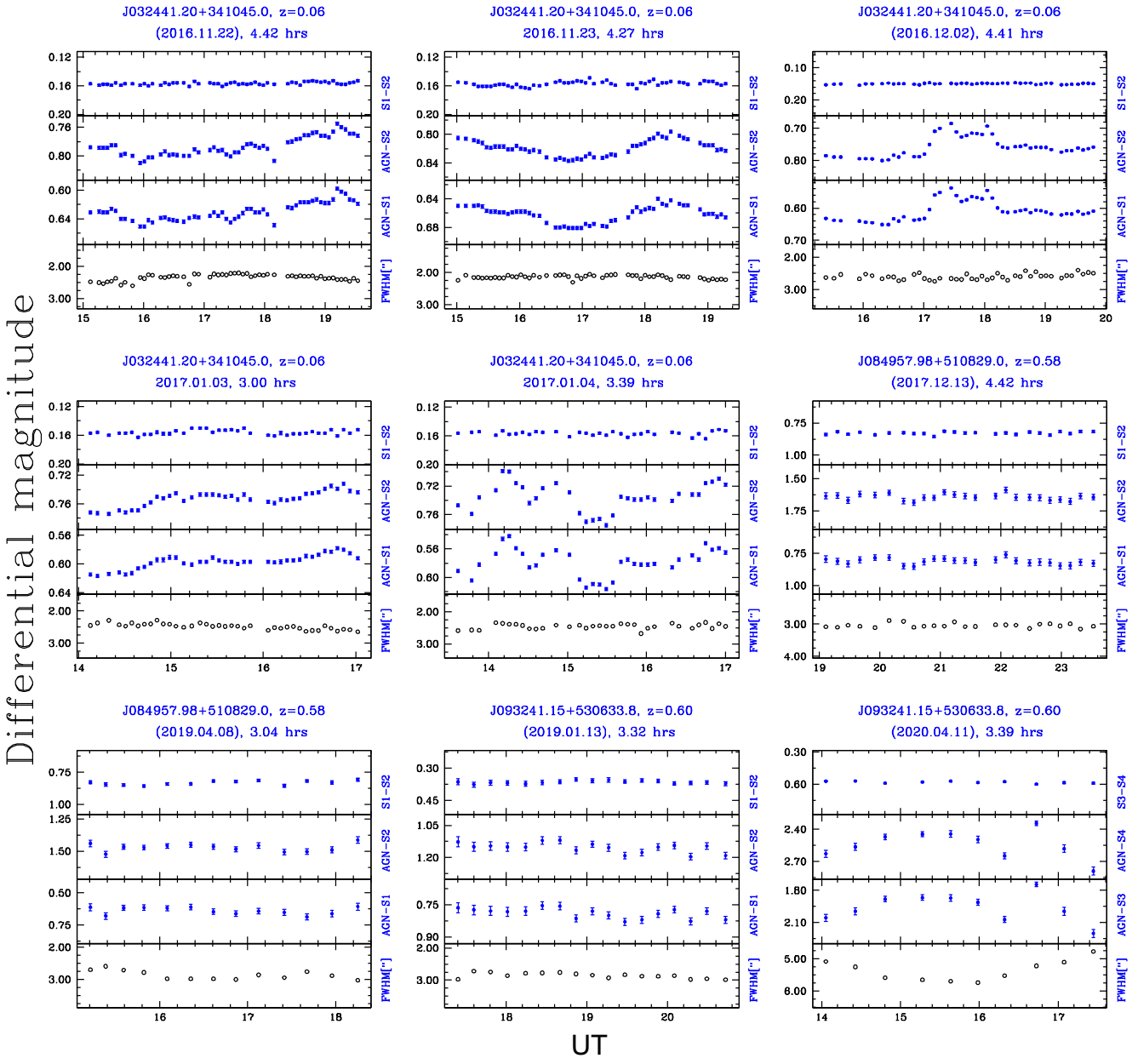

Figure 1. Intra-night differential light curves (DLCs) of the first three γ-ray NLSy1s from our sample of 15 γ-ray NLSy1s. The AGN name, its redshift, and some observational details are given at the top of each panel. The sessions with the date given inside parentheses at the top of each panel were taken for the statistical analysis. In each panel, the upper DLC is derived using the chosen two (non-varying) comparison stars, while the lower two DLCs are the 'NLSy1-star' DLCs, as defined in the labels on the right-hand side. The bottom panel displays the variations of the seeing disc (FWHM) during the monitoring session.

qualitatively different operating conditions of the central engine (Section 1). Another potential difference between these two AGN classes rests on the premise that the jetted NLSy1s represent an earlier stage in the evolution of flat-spectrum quasars/blazars (e.g. Mathur 2000; Sulentic et al. 2000; Mathur, Kuraszkiewicz & Czerny 2001; Fraix-Burnet et al. 2017; Komossa 2018; Paliya 2019).

Out of the total 36 sessions, INOV was significantly detected by both F^{η}-test and the enhanced F-test ($F_{\rm enh}$-test) in 12 sessions. For another 5 sessions, the claim of INOV detection rests on the $F_{\rm enh}$-test alone, while for one session only on the F^{η}-test. Being mindful of this, we shall base our present discussion on the (more conservative) F^{η}-test. Another reason for this stance is that the available INOV information for large sets of blazars also is based on this test (see below). But, before proceeding further, let us revisit the issue, already touched upon in Section 3.2, that the optical aperture photometry of the AGN in some of low-z NLSy1s may have been significantly affected by a (varying) contribution from the host galaxy, in case the seeing disc (PSF) varied during the session. As emphasized by Cellone et al. (2000), under such condition, some DLCs may show statistically significant INOV which is actually spurious (see Section 3.2). As seen from Table 3 and Figs 1–4, data for 29 out of the total 36 sessions have actually been used here for INOV characterization (see Section 4.1). Statistically significant INOV was detected in 13 of the 29 sessions, based on the $F_{\rm enh}$-test and in 10 sessions using the F^{η}-test. Since only the 10 sessions are used here for INOV statistics, we shall presently focus on their DLCs alone,

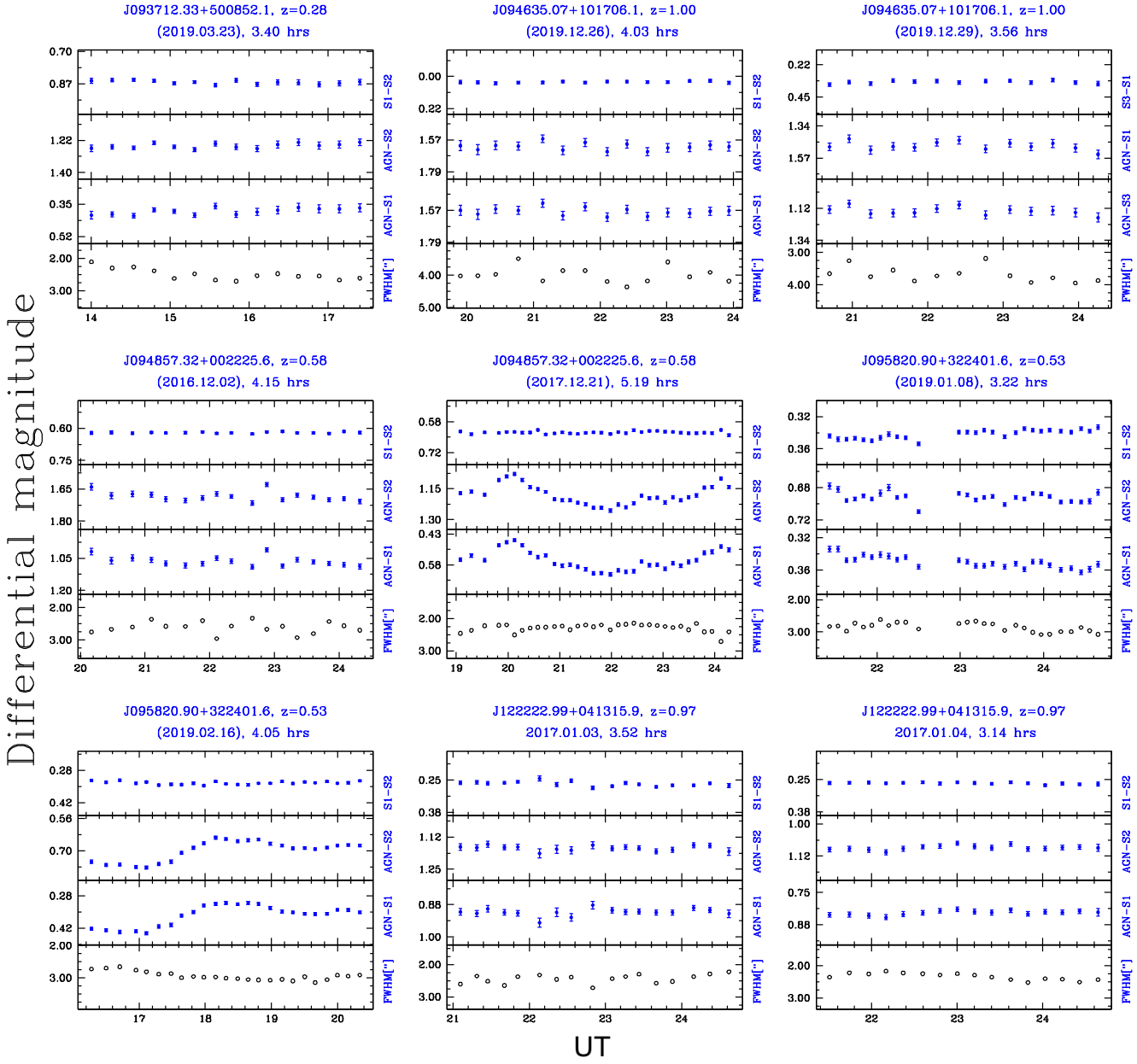

Figure 2. Same as Fig. 1, but for the next 5 γ-ray NLSy1s from our sample of 15 γ-ray NLSy1s galaxies.

from the viewpoint of a possible impact of any PSF variations. From Figs 1–4, it is seen that non-negligible systematic PSF variation occurred in just 4 out of the 10 sessions. Their dates and the target AGNs are 2020 April 11 (J093241.15+530633.8), 2017 February 22, (J122222.99+041315.9), 2019 June 9 (J211852.90–073229.3), and 2019 June 10 (J211817.40+001316.8). A closer inspection of the DLCs of these 4 sessions shows that, except for the one dated 2017 February 22, PSF actually remained fairly steady over the time span when AGN flux showed variation (Figs 1 and 4). Only during the session on 2017 February 22 is the gradient of the DLCs of the target AGN (J122222.99+041315.9) seen to overlap in time with the systematic trend found in the PSF. However, the two gradients are seen to anticorrelate (Fig. 3), which is opposite to what is expected in case the aperture photometric measurements were getting significantly contaminated by the underlying galaxy (see Cellone et al. 2000). Even otherwise, any contamination from the host galaxy can not be significant for this AGN, since its large redshift ($z = 0.97$, Table 1) implies a high intrinsic optical luminosity, enough to swamp the host galaxy. Thus, to sum up, it can be asserted that the inferred INOV detection in neither of the 10 sessions is spurious, and this lends credence to the statistical properties derived using the present data set. This claim is also in accord with the recent high-quality imaging of NLSy1 galaxies by Olguín-Iglesias et al. (2020), as noted in Section 3.2.

The computed INOV DC and amplitudes ($\overline{\psi}$), using our 29 monitoring sessions devoted to the 15 γ-ray NLSy1s, are listed in Table 4. To recall, these are based on the application of the $F_{\rm enh}$ and the F^{η}-tests, adopting a 99 per cent confidence level threshold for confirming INOV detection (Section 4). The two tests have yielded INOV DCs of 39 and 30 per cent, respectively, for our sample. The corresponding estimates using a photometric aperture radius of 3xFWHM (instead of 2xFWHM), for which the DLCs are noisier, are

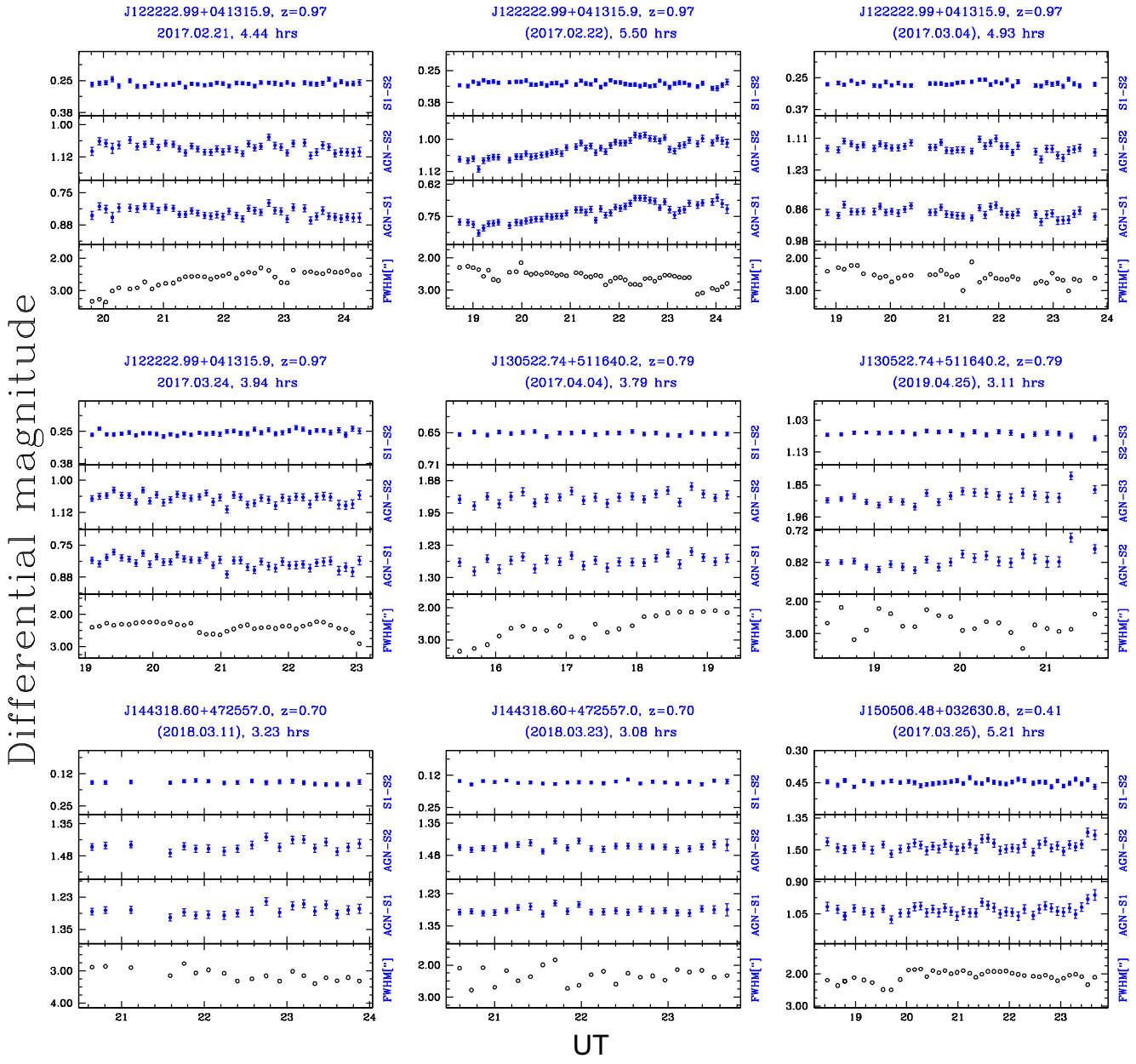

Figure 3. Same as Fig. 1, but for the next 3 γ-ray NLSy1s from our sample of 15 γ-ray NLSy1s galaxies.

found to be 35 and 20 per cent, respectively. Thus, it is realistic to infer that the INOV DC for γ-ray NLSy1s is at least around 25 per cent, based on the F$^{\eta}$-test and around 35–40 per cent using the $F_{\rm enh}$-test. In a systematic study of INOV characteristics of several prominent classes of powerful AGN, based on the F^{η}-test with a confidence level threshold also set at 99 per cent, Goyal et al. (2013) showed that an INOV DC in excess of 20 per cent is observed exclusively for blazar-type objects, i.e. high-optical-polarization quasars, BL Lacs, and TeV detected blazars (see, also Gopal-Krishna et al. 2011), their DC values being about 38, 40, and 47 per cent, respectively. We may recall that, like the present campaign, the monitoring observations leading to these estimates were also made with 1–2 metre class telescopes and a detection threshold of the order of a few per cent was typically achieved. Thus, it seems that, as an AGN class, γ-ray NLSy1s are well matched to blazars in terms of the occurrence rate of INOV, even though their central engines operate in a regime of distinctly higher Eddington accretion rate, as inferred widely in the literature (see Section 1). One interesting consequence of the higher accretion rate for γ-ray NLSy1s is the expected enhancement of the thermal component of the AGN's optical emission, relative to its synchrotron emission (e.g. see Zhou et al. 2007; Paliya et al. 2014). Since the former is likely to be much less variable than the optical flux contributed by the (Doppler boosted) synchrotron jet, the fractional INOV (i.e. INOV amplitude ψ) would be suppressed due to the thermal contamination. The suppression can get compounded due to yet another contaminant, namely the steady optical emission coming from the host galaxy (if detected), which may be significant in the case of low-redshift ($z \lesssim 0.3$) γ-ray NLSy1s harbouring intrinsically much weaker jets than blazars. Some likely implications of both these contaminating/diluting processes have been quantitatively examined recently by Ojha et al. (2019), for the case of the prominent nearby γ-ray NLSy1 galaxy J032441.20+341045.0. The resulting prognosis

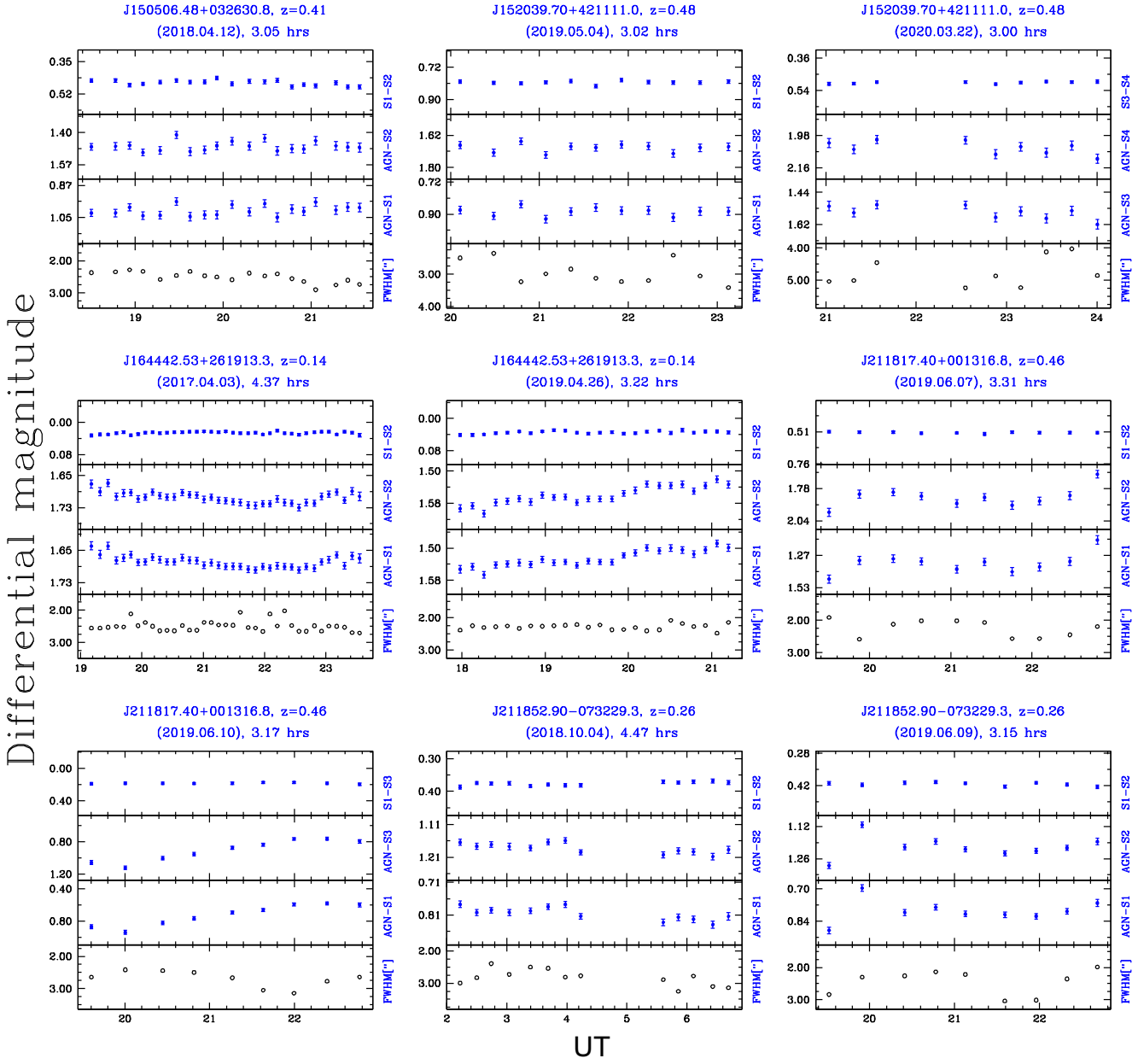

Figure 4. Same as Fig. 1, but for the last 4 γ-ray NLSy1s from our sample of 15 γ-ray NLSy1s galaxies.

in the present context is that future studies of γ-ray NLSy1s may well reveal an even stronger INOV, with a higher DC, once it becomes possible to subtract out the contaminating thermal optical flux originating from the host galaxy and from the processes related to the AGN's inner accretion disc. Thus, it appears that the INOV activity in γ-ray NLSy1s may well turn out to be truly striking, even by the blazar standards.

We now turn attention to any sharp features present in the differential light curves that are linked to the relativistic jet. In various intra-night monitoring campaigns covering dozens of blazars, investigators have searched for brightness changes on time-scales substantially shorter than an hour (e.g. Gopal-Krishna et al. 2011). Such ultra-short time-scales are important since the implied physical size closely approaches the event horizon of a 10^8–10^9 $M_\odot$ black hole (see, also Wiita 2006, Armitage & Reynolds 2003). Indeed, flux variability on minute-like time-scales has been convincingly detected in γ-ray emission from some blazars, e.g. PKS 2155−304 (Aharonian et al. 2007) and PKS 1222+216 (Aleksić et al. 2011). However, several hundred intra-night optical monitoring sessions targeting blazars have yielded just a few claims of INOV on the minute-like time-scale and it is clear that such events are an extremely rare occurrence in blazar light curves (Gopal-Krishna & Wiita 2018; Gopal-Krishna et al. 2019). A remarkable case of sharp optical variation, with an implied *flux doubling time* of just $\sim$ 1 h was observed in our monitoring of the γ-ray NLSy1 galaxy J032441.20+341045.0 on 2016 December 2 (see Fig. 1 for the DLCs). There we had argued that after allowing for the actual dilution by the thermal optical emission, the flux doubling time could be even shorter by a substantial margin, perhaps approaching the minute-like time-scales (Ojha et al. 2019) observed in the γ-ray light curves of some blazars (see above). In that study, we also pointed out that a similarly ultrashort flux doubling time can probably also be

Table 3. Observational details and the inferred INOV status for the sample of 15 γ-ray NLSy1 galaxies (photometric aperture radius used = 2×FWHM).

NLSy1s (SDSS name)	Date(s) yyyy.mm.dd	T (h)	N	Median FWHM (arcsec)	F^{η}-test F_1^{η}, F_2^{η}	INOV status 99 per cent	$F_{\rm enh}$-test $F_{\rm enh}$	INOV status 99 per cent	$\sqrt{\langle\sigma^2_{i,\rm err}\rangle}$ (AGN-s)	$\overline{\psi}_{s1,s2}$ (per cent)	Exposure time for each science frame (s)
(1)	(2)	(3)	(4)	(5)	(6)	(7)	(8)	(9)	(10)	(11)	(12)
J032441.20+341045.0	(2016.11.22)	4.42	56	2.32	14.34, 16.13	V, V	17.39	V	0.003	5.38	240
	2016.11.23	4.27	54	2.13	12.01, 10.69	V, V	05.20	V	0.003	4.07	240
	(2016.12.02)	4.41	44	2.60	85.80, 88.73	V, V	98.29	V	0.003	11.44	300
	2017.01.03	3.00	39	2.47	08.14, 10.55	V, V	03.68	V	0.003	4.02	240
	2017.01.04	3.39	33	2.45	35.03, 35.56	V, V	17.16	V	0.003	7.49	300
J084957.98+510829.0	(2017.12.13)	4.42	24	2.83	00.42, 00.51	NV, NV	00.77	NV	0.033	–	600
	(2019.04.08)	3.04	13	2.88	00.66, 00.89	NV, NV	00.62	NV	0.032	–	840
J093241.15+530633.8	(2019.01.13)	3.32	17	2.86	00.80, 00.81	NV, NV	04.09	V	0.027	6.59	720
	(2020.04.11)	3.39	10	5.24	07.94, 08.10	V, V	07.94	V	0.046	44.64	1080
J093712.33+500852.1	(2019.03.23)	3.40	14	2.54	00.43, 00.33	NV, NV	01.46	NV	0.025	–	900
J094635.07+101706.1	(2019.12.26)	4.03	14	4.02	00.30, 00.34	NV, NV	02.72	NV	0.045	–	1020
	(2019.12.29)	3.56	13	3.73	00.54, 00.42	NV, NV	01.64	NV	0.041	–	900
J094857.32+002225.6	(2016.12.02)	4.15	17	2.58	01.71, 01.88	NV, NV	10.52	V	0.017	7.95	780
	(2017.12.21)	5.19	33	2.24	13.95, 16.53	V, V	25.26	V	0.012	16.42	540
J095820.90+322401.6	(2019.01.08)	3.22	27	2.81	02.80, 03.00	V, V	01.17	NV	0.004	3.00	360
	(2019.02.16)	4.05	24	2.97	21.15, 21.86	V, V	24.90	V	0.009	12.98	540
J122222.99+041315.9	2017.01.03	3.52	17	2.38	00.62, 00.30	NV, NV	00.68	NV	0.018	–	600
	2017.01.04	3.14	16	2.36	00.32, 00.37	NV, NV	01.99	NV	0.014	–	720
	2017.02.21	4.44	41	2.65	00.74, 00.76	NV, NV	02.13	V	0.020	6.36	360
	(2017.02.22)	5.50	50	2.59	03.98, 03.60	V, V	06.51	V	0.017	13.33	360
	(2017.03.04)	4.93	39	2.61	00.72, 00.86	NV, NV	01.36	NV	0.019	–	360
	2017.03.24	3.94	39	2.37	00.93, 00.75	NV, NV	01.66	NV	0.020	–	360
J130522.75+511640.2	(2017.04.04)	3.79	23	2.57	00.66, 00.70	NV, NV	02.94	PV	0.012	–	600
	(2019.04.25)	3.11	22	2.77	01.42, 01.56	NV, NV	04.12	PV	0.018	–	480
J144318.56+472556.7	(2018.03.11)	3.23	19	3.15	00.56, 00.54	NV, NV	02.59	NV	0.022	–	480
	(2018.03.23)	3.08	23	2.33	00.36, 00.35	NV, NV	01.00	NV	0.018	–	480
J150506.48+032630.8	(2017.03.25)	5.21	41	2.08	00.60, 00.59	NV, NV	01.04	NV	0.028	–	420
	(2018.04.12)	3.05	19	2.55	00.67, 00.63	NV, NV	00.84	NV	0.032	–	480
J152039.70+421111.0	(2019.05.04)	3.02	11	3.08	00.56, 00.61	NV, NV	01.43	NV	0.031	–	900
	(2020.03.22)	3.00	09	4.85	01.00, 01.00	NV, NV	03.69	NV	0.034	–	900
J164442.53+261913.3	(2017.04.03)	4.37	37	2.50	01.44, 01.28	NV, NV	03.53	V	0.011	5.41	420
	(2019.04.26)	3.22	24	2.27	03.06, 03.74	V, V	06.40	V	0.011	7.50	480
J211817.40+001316.8	(2019.06.07)	3.31	10	2.19	03.00, 03.08	NV, NV	26.26	V	0.046	29.75	1200
	(2019.06.10)	3.17	09	2.64	16.38, 18.42	V, V	144.97	V	0.032	35.57	1200
J211852.90–073229.3	(2018.10.04)	4.47	13	2.81	01.87, 01.26	NV, NV	03.47	NV	0.014	–	900
	(2019.06.09)	3.15	09	2.30	06.38, 06.55	V, V	12.31	V	0.019	17.85	1200

The columns are as follows: (1) SDSS name of the NLSy1; (2) date(s) of the monitoring session(s). Dates inside parentheses are for the longest two sessions which we have used for estimating the INOV duty cycle (DC); (3) duration of the monitoring session; (4) number of data points in the DLCs for the monitoring session; (5) median seeing (FWHM in arcsec) for the session; (6) F-values for the two DLCs (relative to the two comparison stars), based on the F^{η}-test; (7) INOV status inferred from the two DLCs, using the F^{η}-test, with V = variable (confidence level ≥99 per cent), PV = probable variable (confidence level between 95 and 99 per cent), NV = non-variable (confidence level < 95 per cent); (8) F-values for the 'NLSy1-reference star' DLC, based on the $F_{\rm enh}$-test; (9) INOV status inferred using the $F_{\rm enh}$-test; (10) mean photometric error for the two DLCs of the target AGN relative to the two comparison stars; (11) mean amplitude of variability in the two DLCs; and (12) exposure time per frame in the DLC.

Table 4. The DC and $\overline{\psi}$ of INOV, computed for the present sample of 15 γ-ray NLSy1 galaxies, based on the $F_{\rm enh}$-test and F^{η}-test.

	Based on the $F_{\rm enh}$-test		Based on the F^{η}-test	
γ-ray NLSy1s	[a]DC (per cent)	$^a\overline{\psi}^b$ (per cent)	[a]DC (per cent)	$^a\overline{\psi}^b$ (per cent)
	39	16	30	17

Notes. [a]Only using the 29 sessions, as explained in Section 4.1.
[b]This is the mean value for all the DLCs belonging to the type 'V'.

inferred from this AGN's already existing intra-night DLCs dated 2012 December 9, published in Paliya et al. (2014) and, secondly, that such extremely rapid events may be correlated with the radio jet's superluminal speed (Ojha et al. 2019). Here we note that radio jets showing superluminal speeds have been shown to exist in five members of the present sample of 15 γ-ray NLSy1s. These five sources are J032441.20+341045.0, J122222.99+041315.9, J150506.48+032630.8, with v_{app}/c of 9.1 ± 0.3 and 0.9 ± 0.3, 1.1 ± 0.4, respectively (e.g. see Lister et al. 2016), and J084957.98+510829.0, J094857.32+002225.6 having v_{app}/c of 6.6 ± 0.8 and 9.1 ± 0.3, respectively (e.g. see Lister et al. 2019). Optical flux variability on minute to hour-like time-scales has also been reported for these five γ-ray NLSy1s (Liu et al. 2010; Paliya et al. 2013a, 2016; Ojha et al. 2019). The possibility of such a correlation could be firmly tested when the more extensive INOV data base and superluminal speeds of the jets become available for γ-ray NLSy1s. In the present campaign, we have searched for additional clean examples of variability on time-scales $\ll$ 1 h (see Figs 1–4). As explained below, only two such events could be identified, although some more may well be found when DLCs with comparably dense sampling become available for our entire sample.

From Fig. 1, one of the two events is associated, once again, with J032441.20+341045.0 ($z = 0.06$), when roughly in the middle of its

3.4-h-long monitoring session on 2017 January 4, i.e. around 15:00 UT, its flux underwent a sharp drop by $\sim$ 3 per cent within $\sim$ 6 min and then, after remaining stagnant for $\sim$20 min, the flux jumped back by $\sim$3 per cent within 6 min. Now, following the arguments made by us previously in Ojha et al. (2019) and recalled earlier in this section, the actual amplitude of both these flux changes are likely to be several times greater once a correction is made for the dilution of the jet's optical emission, due to the (much steadier) thermal emission contributed by this strongly accreting AGN itself and also by its host galaxy. It is also interesting to note that out of the total 10 monitoring sessions of >3-h duration, reported for this AGN here (five sessions) and in previous studies (Paliya et al. 2013a, 2014; Ojha et al. 2019), strong features of duration $\ll$1 h have been observed in the DLCs of as many as three sessions. Thus, large and ultra-fast brightness changes appear to be a remarkable behavioural signature of this γ-ray NLSy1 galaxy! Moving now to the second large event of comparable sharpness, found in the present data set, it can be seen in the DLCs of the source J094857.32+002225.8 (z = 0.584) on 2017 December 21. During that 5.2-h-long monitoring session (Fig. 2), at around 19.55 UT, the flux showed a sharp jump (between two consecutive points) of $\sim$7 per cent within $\sim$15 min. Although, for this source, no estimates are currently available for the dilution by thermal optical emission, such a contamination is quite likely (especially from the AGN accretion disc), going by the above-mentioned example of the γ-ray NLSy1 J032441.20+341045.0. Note that a very strong INOV of J094857.32+002225.8 has been reported previously in the independent campaigns conducted by Liu et al. (2010) and Maune et al. (2013). The most rapid flux evolution, found by the latter team, occurred on 2011 April 1 and amounted to a rate of 0.2–0.3 mag h^{-1}. Thus, both these γ-ray NLSy1s are proto-types of blazar-like jet activity, probably even surpassing them in the rapidity of brightness change. It is also interesting to note that these two AGN, although grossly different in redshift, display highly superluminal nuclear radio jets, with a speed of up to 7c in case of J032441.20+341045.0 (Fuhrmann et al. 2016) and 9c for J094857.32+002225.6 (Lister et al. 2019). Thus, in summary, the fact that in the present large and unbiased sample of γ-ray NLSy1s, at least 2 out of total 29 sessions have an event with optical flux doubling time of $\lesssim$1 h. In contrast, such rapid optical variations have hardly ever been observed in the extensive monitoring programs targetting blazars (see above). Could the contrast be a reflection of the qualitative physical differences between the central engines of these two types of jetted AGNs (Section 1)? This appears to be a potentially important emerging clue, to be probed by further observations.

6 CONCLUSIONS

Although the first INOV observations of a γ-ray NLSy1 galaxy were reported a decade ago (Liu et al. 2010), subsequent follow-up has been limited to just six members of this intriguing class of AGN. This study, based on a much larger sample (see below) is the first attempt to systematically characterize the INOV properties of γ-ray NLSy1 galaxies. These jetted AGNs are particularly interesting since their central engines are thought to operate in a physical regime of accretion rate different from what is believed to occur in (more powerful) blazars. Our study is based on an unbiased sample of 15 γ-ray NLSy1s, assembled by applying well-defined selection criteria to a total of 20 such objects known at present. Based on their monitoring in 36 sessions of minimum 3-h duration, we estimate an INOV DC of 25–30 per cent for a typical INOV amplitude detection threshold of around 3–5 per cent. Among the powerful AGNs, only blazars are known to achieve INOV DC exceeding $\sim$20 per cent. Thus, as a class, γ-ray NLSy1s resemble blazars even in INOV properties. As discussed in Section 5, it is quite likely that we may have underestimated the DC for γ-ray NLSy1s because their nonthermal optical emission which is primarily responsible for INOV, could be significantly diluted by the much less variable optical emission contributed by the host galaxy (in case of lower redshift sources) and the accretion disc operating at a high Eddington accretion rate (Boroson & Green 1992; Pounds, Done & Osborne 1995; Sulentic et al. 2000; Boroson 2002; Collin & Kawaguchi 2004; Grupe & Mathur 2004; Paliya 2019; Ojha et al. 2020a).

Further, we have detected in the light curves of two prominent members of our sample of 15 γ-ray NLSy1s, ultrarapid brightness changes amounting to a clear level change within $\sim$0.1 h. Quite plausibly, with a similarly dense sampling of the light curves for our entire sample, more such events would be found. But already, this result seems to stand in contrast to the observed extreme rarity of such distinct ultra-rapid events of optical variability in blazar light curves, even though they vastly outnumber the light curves currently available for γ-ray NLSy1s. If this difference is firmly established by further observations of γ-ray NLSy1s, that would provide a useful input to the models of jet formation in these enigmatic AGNs.

ACKNOWLEDGEMENTS

We thank an anonymous referee for his/her very important comments that helped us to improve this paper considerably. We also thank the concerned ARIES staff for assistance during the observations. G-K thanks the Indian National Science Academy for a Senior Scientist fellowship.

DATA AVAILABILITY

The data used in this paper are from 1.3-m Devasthal Fast Optical Telescope (DFOT) of Aryabhatta Research Institute of Observational Sciences (ARIES), Nainital, India (https://www.aries.res.in/facilities/astronomical-telescopes/13m-telescope), which will be shared on reasonable request to the corresponding author.

REFERENCES

Abdo A. A. et al., 2009a, ApJ, 699, 976
Abdo A. A. et al., 2009b, ApJ, 707, 727
Abdo A. A. et al., 2009c, ApJ, 707, L142
Abdollahi S. et al., 2020, ApJS, 247, 33
Abolfathi B. et al., 2018, ApJS, 235, 42
Aharonian F. et al., 2007, ApJ, 664, L71
Aleksić J. et al., 2011, ApJ, 730, L8
Armitage P. J., Reynolds C. S., 2003, MNRAS, 341, 1041
Bai J. M., Xie G. Z., Li K. H., Zhang X., Liu W. W., 1999, A&AS, 136, 455
Berton M. et al., 2018, A&A, 614, A87
Boller T., Brandt W. N., Fink H., 1996, A&A, 305, 53
Boroson T. A., 2002, ApJ, 565, 78
Boroson T. A., Green R. F., 1992, ApJS, 80, 109
Calderone G., Ghisellini G., Colpi M., Dotti M., 2013, MNRAS, 431, 210
Camenzind M., Krockenberger M., 1992, A&A, 255, 59
Carini M. T., 1990, PhD thesis, George State Univ.
Carini M. T., Miller H. R., Noble J. C., Goodrich B. D., 1992, AJ, 104, 15
Carini M. T., Noble J. C., Miller H. R., 2003, AJ, 125, 1811
Carini M. T., Noble J. C., Taylor R., Culler R., 2007, AJ, 133, 303
Cellone S. A., Romero G. E., Combi J. A., 2000, AJ, 119, 1534
Cellone S. A., Romero G. E., Araudo A. T., 2007, MNRAS, 374, 357
Chakrabarti S. K., Wiita P. J., 1993, ApJ, 411, 602
Chand H., Kumar P., Gopal-Krishna, 2014, MNRAS, 441, 726

Ciprini S., Fermi-LAT Collaboration, 2018, Proc. Sci., Revisiting Narrow-Line Seyfert 1 Galaxies and their Place in the Universe. SISSA, Trieste, PoS#020
Collin S., Kawaguchi T., 2004, A&A, 426, 797
Cracco V., Ciroi S., Berton M., Di Mille F., Foschini L., La Mura G., Rafanelli P., 2016, MNRAS, 462, 1256
Czerny B., Siemiginowska A., Janiuk A., Gupta A. C., 2008, MNRAS, 386, 1557
D'Ammando F. et al., 2012, MNRAS, 426, 317
D'Ammando F., Orienti M., Larsson J., Giroletti M., 2015, MNRAS, 452, 520
de Diego J. A., 2010, AJ, 139, 1269
de Diego J. A., 2014, AJ, 148, 93
Decarli R., Dotti M., Fontana M., Haardt F., 2008, MNRAS, 386, L15
Deo R. P., Crenshaw D. M., Kraemer S. B., 2006, AJ, 132, 321
Fan J. H., Qian B. C., Tao J., 2001, A&A, 369, 758
Ferrara E. C., Miller H. R., McFarland J. P., Williams A. M., Wilson J. W., Fried R. E., Noble J. C., 2001, in Peterson B. M., Pogge R. W., Polidan R. S., eds, ASP Conf. Ser. Vol. 224, Probing the Physics of Active Galactic Nuclei. Astron. Soc. Pac., San Francisco, p. 319
Foschini L., 2011, Proc. Sci., Narrow-Line Seyfert 1 Galaxies and their Place in the Universe. SISSA, Trieste, PoS#024
Foschini L., Fermi/Lat Collaboration, Ghisellini G., Maraschi L., Tavecchio F., Angelakis E., 2010, in Maraschi L., Ghisellini G., Della Ceca R., Tavecchio F., eds, ASP Conf. Ser. Vol. 427, Accretion and Ejection in AGN: A Global View. Astron. Soc. Pac., San Francisco, p. 243
Foschini L. et al., 2015, A&A, 575, A13
Fraix-Burnet D., Marziani P., D'Onofrio M., Dultzin D., 2017, Frontiers Astron. Space Sci., 4, 1
Fuhrmann L. et al., 2016, Res. Astron. Astrophys., 16, 176
Ganci V., Marziani P., D'Onofrio M., del Olmo A., Bon E., Bon N., Negrete C. A., 2019, A&A, 630, A110
Goodrich R. W., Stringfellow G. S., Penrod G. D., Filippenko A. V., 1989, ApJ, 342, 908
Gopal-Krishna, Wiita P. J., 1992, A&A, 259, 109
Gopal-Krishna, Wiita P. J., 2018, Bull. Soc. R. Sci. Liege, 87, 281
Gopal-Krishna, Wiita P. J., Altieri B., 1993, A&A, 271, 89
Gopal-Krishna, Sagar R., Wiita P. J., 1995, MNRAS, 274, 701
Gopal-Krishna, Stalin C. S., Sagar R., Wiita P. J., 2003, ApJ, 586, L25
Gopal-Krishna, Goyal A., Joshi S., Karthick C., Sagar R., Wiita P. J., Anupama G. C., Sahu D. K., 2011, MNRAS, 416, 101
Gopal-Krishna, Joshi R., Chand H., 2013, MNRAS, 430, 1302
Gopal-Krishna, Britzen S., Wiita P., 2019, Bull. Soc. R. Sci. Liege, 88, 132
Goyal A., Gopal-Krishna, Wiita P. J., Anupama G. C., Sahu D. K., Sagar R., Joshi S., 2012, A&A, 544, A37
Goyal A., Gopal-Krishna, Paul J. W., Stalin C. S., Sagar R., 2013, MNRAS, 435, 1300
Grupe D., Mathur S., 2004, ApJ, 606, L41
Grupe D., Beuermann K., Thomas H.-C., Mannheim K., Fink H. H., 1998, A&A, 330, 25
Gupta A. C., Joshi U. C., 2005, A&A, 440, 855
Heidt J., Wagner S. J., 1996, A&A, 305, 42
Howell S. B., 1989, PASP, 101, 616
Howell S. B., Warnock III A., Mitchell K. J., 1988, AJ, 95, 247
Hughes P. A., Aller H. D., Aller M. F., 1991, ApJ, 374, 57
Itoh R. et al., 2013, ApJ, 775, L26
Jang M., Miller H. R., 1995, ApJ, 452, 582
Joshi R., Chand H., Gupta A. C., Wiita P. J., 2011, MNRAS, 412, 2717
Kellermann K. I., Sramek R., Schmidt M., Shaffer D. B., Green R., 1989, AJ, 98, 1195
Kellermann K. I., Sramek R. A., Schmidt M., Green R. F., Shaffer D. B., 1994, AJ, 108, 1163
Kellermann K. I., Condon J. J., Kimball A. E., Perley R. A., Ivezić Ž., 2016, ApJ, 831, 168
Klimek E. S., Gaskell C. M., Hedrick C. H., 2004, ApJ, 609, 69
Komossa S.,2018, Proc. Sci., Revisiting Narrow-Line Seyfert 1 Galaxies and their Place in the Universe. SISSA, Trieste, PoS#015
Komossa S., Meerschweinchen J., 2000, A&A, 354, 411
Komossa S., Voges W., Xu D., Mathur S., Adorf H.-M., Lemson G., Duschl W. J., Grupe D., 2006, AJ, 132, 531
Kshama S. K., Paliya V. S., Stalin C. S., 2017, MNRAS, 466, 2679
Kumar P., Gopal-Krishna, Chand H., 2015, MNRAS, 448, 1463
Kumar P., Chand H., Gopal-Krishna, 2016, MNRAS, 461, 666
Kumar P., Gopal-Krishna, Stalin C. S., Chand H., Srianand R., Petitjean P., 2017, MNRAS, 471, 606
Leighly K. M., 1999, ApJS, 125, 297
Lister M., 2018, Proc. Sci., Revisiting Narrow-Line Seyfert 1 Galaxies and their Place in the Universe. SISSA, Trieste, PoS#022
Lister M. L. et al., 2016, AJ, 152, 12
Lister M. L. et al., 2019, ApJ, 874, 43
Liu H., Wang J., Mao Y., Wei J., 2010, ApJ, 715, L113
Mangalam A. V., Wiita P. J., 1993, ApJ, 406, 420
Marconi A., Axon D. J., Maiolino R., Nagao T., Pastorini G., Pietrini P., Robinson A., Torricelli G., 2008, ApJ, 678, 693
Marscher A. P., 1996, in Miller H. R., Webb J. R., Noble J. C., eds, ASP Conf. Ser. Vol. 110, Blazar Continuum Variability. Astron. Soc. Pac., San Francisco, p. 248
Marscher A. P., Gear W. K., 1985, ApJ, 298, 114
Mathur S., 2000, MNRAS, 314, L17
Mathur S., Kuraszkiewicz J., Czerny B., 2001, New Astron., 6, 321
Maune J. D., Miller H. R., Eggen J. R., 2013, ApJ, 762, 124
Miller H. R., Carini M. T., Goodrich B. D., 1989, Nature, 337, 627
Miller H. R., Ferrara E. C., McFarland J. P., Wilson J. W., Daya A. B., Fried R. E., 2000, New Astron. Rev., 44, 539
Monet D. G., 1998, BAAS, 30, 1427
Ojha V., Chand H., Gopal-Krishna, 2018, Bull. Soc. R. Sci. Liege, 87, 387
Ojha V., Gopal-Krishna, Chand H., 2019, MNRAS, 483, 3036
Ojha V., Chand H., Dewangan G. C., Rakshit S., 2020a, ApJ, 896, 95
Ojha V., Chand H., Gopal-Krishna, Mishra S., Chand K., 2020b, MNRAS, 493, 3642
Olguín-Iglesias A., Kotilainen J., Chavushyan V., 2020, MNRAS, 492, 1450
Osterbrock D. E., Pogge R. W., 1985, ApJ, 297, 166
Paliya V. S., 2019, J. Astrophys. Astron., 40, 39
Paliya V. S., Stalin C. S., Kumar B., Kumar B., Bhatt V. K., Pandey S. B., Yadav R. K. S., 2013a, MNRAS, 428, 2450
Paliya V. S., Stalin C. S., Shukla A., Sahayanathan S., 2013b, ApJ, 768, 52
Paliya V. S., Sahayanathan S., Parker M. L., Fabian A. C., Stalin C. S., Anjum A., Pandey S. B., 2014, ApJ, 789, 143
Paliya V. S., Rajput B., Stalin C. S., Pandey S. B., 2016, ApJ, 819, 121
Paliya V. S., Ajello M., Rakshit S., Mandal A. K., Stalin C. S., Kaur A., Hartmann D., 2018, ApJ, 853, L2
Paliya V. S., Parker M. L., Jiang J., Fabian A. C., Brenneman L., Ajello M., Hartmann D., 2019, ApJ, 872, 169
Peterson B. M., 2011, Proc. Sci., Narrow-Line Seyfert 1 Galaxies and their Place in the Universe. SISSA, Trieste, PoS#032
Peterson B. M. et al., 2000, ApJ, 542, 161
Pogge R. W., 2011, Proc. Sci., Narrow-Line Seyfert 1 Galaxies and their Place in the Universe. SISSA, Trieste, PoS#002
Pounds K. A., Done C., Osborne J. P., 1995, MNRAS, 277, L5
Qian S. J., Quirrenbach A., Witzel A., Krichbaum T. P., Hummel C. A., Zensus J. A., 1991, A&A, 241, 15
Rakshit S., Stalin C. S., Chand H., Zhang X.-G., 2017, ApJS, 229, 39
Ramírez A., de Diego J. A., Dultzin D., González-Pérez J.-N., 2009, AJ, 138, 991
Romero G. E., Cellone S. A., Combi J. A., 1999, A&AS, 135, 477
Sagar R., Kumar B., Omar A., Pandey A. K., 2010, in Ojha D. K., ed., ASP Conf. Ser. Vol. 1, Interstellar Matter and Star Formation: A Multi-wavelength Perspective. Astron. Soc. Pac., San Francisco, p. 203
Shuder J. M., Osterbrock D. E., 1981, ApJ, 250, 55
Singh V., Chand H., 2018, MNRAS, 480, 1796
Stalin C. S., Gopal-Krishna, Sagar R., Wiita P. J., 2004, MNRAS, 350, 175
Stetson P. B., 1987, PASP, 99, 191
Stetson P. B., 1992, in Worrall D. M., Biemesderfer C., Barnes J., eds, ASP Conf. Ser. Vol. 25, Astronomical Data Analysis Software and Systems I. Astron. Soc. Pac., San Francisco, p. 297
Stocke J. T., Morris S. L., Weymann R. J., Foltz C. B., 1992, ApJ, 396, 487

Sulentic J. W., Zwitter T., Marziani P., Dultzin-Hacyan D., 2000, ApJ, 536, L5
Ulrich M.-H., Maraschi L., Urry C. M., 1997, ARA&A, 35, 445
Urry C. M., Padovani P., 1995, PASP, 107, 803
Visnovsky K. L., Impey C. D., Foltz C. B., Hewett P. C., Weymann R. J., Morris S. L., 1992, ApJ, 391, 560
Viswanath G., Stalin C. S., Rakshit S., Kurian K. S., Ujjwal K., Gudennavar S. B., Kartha S. S., 2019, ApJ, 881, L24
Wagner S. J., Witzel A., 1995, ARA&A, 33, 163
Wang T., Brinkmann W., Bergeron J., 1996, A&A, 309, 81
Wiita P. J., 2006, in Miller H. R., Marshall K., Webb J. R., Aller M. F., eds, ASP Conf. Ser. Vol. 350, Blazar Variability Workshop II: Entering the GLAST Era. Astron. Soc. Pac., San Francisco, p. 183
Yang H. et al., 2018, MNRAS, 477, 5127
Yao S., Yuan W., Zhou H., Komossa S., Zhang J., Qiao E., Liu B., 2015, MNRAS, 454, L16
Yao S., Komossa S., Liu W.-J., Yi W., Yuan W., Zhou H., Wu X.-B., 2019, MNRAS, 487, L40
Yuan W., Zhou H. Y., Komossa S., Dong X. B., Wang T. G., Lu H. L., Bai J. M., 2008, ApJ, 685, 801
Zensus J. A., 1997, ARA&A, 35, 607
Zhou H., Wang T., Yuan W., Lu H., Dong X., Wang J., Lu Y., 2006, ApJS, 166, 128
Zhou H. et al., 2007, ApJ, 658, L13
Zhou H.-Y., Wang T.-G., 2002, Chin. J. Astron. Astrophys., 2, 501

This paper has been typeset from a TEX/LATEX file prepared by the author.